Volume 1 | Number 1 | Jan 2013 | Pages 1–100

ChemComm

Chemical Communications
www.rsc.org/chemcomm

ROYAL SOCIETY OF CHEMISTRY

This is an *Accepted Manuscript*, which has been through the Royal Society of Chemistry peer review process and has been accepted for publication.

Accepted Manuscripts are published online shortly after acceptance, before technical editing, formatting and proof reading. Using this free service, authors can make their results available to the community, in citable form, before we publish the edited article. We will replace this *Accepted Manuscript* with the edited and formatted *Advance Article* as soon as it is available.

You can find more information about *Accepted Manuscripts* in the **Information for Authors**.

Please note that technical editing may introduce minor changes to the text and/or graphics, which may alter content. The journal's standard **Terms & Conditions** and the **Ethical guidelines** still apply. In no event shall the Royal Society of Chemistry be held responsible for any errors or omissions in this *Accepted Manuscript* or any consequences arising from the use of any information it contains.

Journal Name

COMMUNICATION

The performance and stability of oxygen reduction reaction on Pt-M (M=Pd, Ag and Au) nanorods: An experimental and computational study

Yu-Ting Liang,[a] Syuan-Pei Lin,[b] Chen-Wei Liu,[c] Shu-Ru Chung,[d] Tsan-Yao Chen,[e] Jeng-Han Wang [b,*] and Kuan-Wen Wang [a,*]

The ORR activity of Pt₃M NRs is related to the oxophilicity (ΔE_{ads}). However, their segregation energy when exposing to oxygen containing species (OCS*) determines the stability. Although the ΔE_{ads} of Ag is not as weak as Au, its structure is relative stable, promoting the ORR stability.

The development of Pt-based catalysts towards oxygen reduction reaction (ORR) for polymer electrolyte membrane fuel cells (PEMFCs) has attracted much attention through control of the morphologies, alloying components, and structures.[1] By applying density functional theory (DFT) calculation, Pt alloying with transition metals like Mn, Fe, Co, Ni, Pd and Ru with delicate structures have been screened to find the potential catalysts with high ORR performance exceeding Pt alone.[2] Recent study shows that the incorporation of submonolayer M (M = Mn, Fe, Co, and Ni) into Pt(111) result in the enhancement of ORR activity.[2a-2d] These transition metals in the subsurface layer soften the chemical bonding between Pt and the oxygen-containing species (OCS*) due to the suppression of Pt surface-states near the Fermi level.[2b] Basically, absorption energies of OCS*, specifically, O* and OH*, are used as indicators for ORR activity, where a weaker or more positive energy can promote the ORR activity. Moreover, the stability of cathode catalysts under ORR operation can be verified from the calculation of segregation energy. Both adsorption and segregation energies, thus, are rather important to justify materials with the better ORR activity and stability.[2a] Previous studies extensively examined these energetics on Pt alloying with 3d transition metals, e.g. Sc to Ni, or neighboring Pd; however, the late transition metals, such as Ag and Au, which also showed good ORR activity,[3] have seldom been investigated.

In this study, we have investigated the ORR activity and stability of Pt₃M (M= Au, Ag, and Pd) nanorods (NRs), which have potentially good activity and stability, experimentally and computationally. The Pt₃M NRs with an aspect ratio of 4.0 are prepared by a novel and simple formic acid reduction method. DFT calculation at the GGA-PW91 level[4] with a 3D periodic boundary condition implemented in Vienna Ab initio Simulation Package (VASP)[5] has been used in the present study. The computed adsorption energy (E_{ads}) of OCS* for various PtM materials is related to the ORR performance while the segregation energy for clean (E_{seg}(clean)) and Pt-OCS* (E_{seg}(OCS*)) surfaces can be used to predict the stability of the NRs. We believe that this is the first time that those Pt₃M NRs has been elucidated comprehensively. Besides, we have investigated that although the oxophilicity of Pt is well-modified by Au, due to the significant Pt surface segregation when exposing to OCS*, the PtAu NRs cannot retain their high activity after long term test. On the other hand, PtAg with moderate oxophilicity and relative stable structure when contacting with OCS* has the smallest decay rate after accelerated durability test (ADT).

Figure 1(a), (b) and (c) show the morphologies of the as-prepared catalysts analyzed by high resolution transmission electron microscopy (HR-TEM). The NRs with an aspect ratio about 4.0 and a diameter of 3-5 nm are well-dispersed on the carbon support. After 1000 cycles of ADT, as shown in Figure 1(d)-(f), different degrees of Pt aggregation, migration and carbon corrosion occur and rod-like structure can be still observed, suggesting that the NRs structure and alloying can lessen the effect of dissolution, Ostwald ripening and aggregation of the catalysts in acidic conditions when compared to carbon-supported nanoparticles.[6] Moreover, since the NRs are prepared by reduction of Pt first and then deposition of M latter, a core/shell like structure (Pt@M) with the Pt/M atomic ratio of 3 is obtained as evidenced by the extended X-Ray absorption fine structure (EXAFS) results exhibited in Figures S1 and S2, and compositional and fitting results listed in Tables S1 and S2 in the Supporting Information (SI).[1a,6a] Moreover, the X-ray diffraction (XRD) patterns of Pt₃M NRs are shown in Figure S3 in SI. The peak areas integrated from (111), (200), and (220) planes for various NRs are calculated and used to describe the degrees of anisotropic growth, which influence the ORR performance significantly. As listed in Table S1 in SI, the peak area ratios of [(111)+(220)/(200)] for NRs are all higher than that for carbon-supported Pt nanoparticles (Pt/C, 46 % from TKK),[1a] suggesting a promoted ORR performance. Moreover, due to the pronounced (111) anisotropic growth, the DFT are modeled on the (111) facets to examine the catalytic trends on Pt-based alloys.

Figure S4 in SI displays the temperature-programmed reduction (TPR) results of NRs, which can reflect the species of the topmost surface by using the hydrogen consumption peak temperature of chemisorbed oxygen on the catalysts.[7] The representative species for NRs are also marked in Figure S4. Peak temperatures located at about 240 and 300 K represent the reduction peaks of PtO and PtO₂,

respectively. It seems that the deposition of Au can modify the Pt surface so that besides peaks belonging to PtO_x and AuO_x, a peak located at 220 K owing to the reduction of chemisorbed oxygen on PtAu alloy is noted.[7a,7b] On the other hand, for PtPd and PtAg NRs, the peak attributed to the reduction of chemisorbed oxygen on alloys is located at 280 and 290 K, respectively. The above TPR results suggest that the modification of oxophilicity for Pt surface by alloying has the trend of Au > Ag > Pd. Surface Au in the Pt alloy with weaker oxygen binding energy can lower the oxophilicity, thus promoting its ORR performance.[3] On the other hand, the surface Pt compositions for various NRs are characterized by X-ray photoelectron spectroscopy (XPS) and shown in Figure S5. It seems that consistent with the TPR results, the surface composition of metallic Pt is enhanced due to the alloying of Au.

Figure 2 compares the linear sweep voltammetry (LSV) of NRs before and after ADT. The mass activity (MA), obtained by the normalization of the kinetic current density to the Pt loading, is 117.2, 102.7, 103.1, and 90.0 mA cm^{-2} at 0.85 V of PtAu, PtPd, PtAg, and Pt/C, respectively as listed in Table S1. Moreover, the stability of various catalysts measured by ADT and shown in Figure 2 clearly demonstrate that PtAg has the best stability with the highest MA and a smallest decay of 9 % as listed in Table S1, when compared to a decay of 71 % for Pt/C. It is interesting to mention that although PtAu has the best ORR performance in the first cycle, its stability is not as good as PtAg.

DFT calculation is performed to further reveal catalytic mechanism in the experimental observation. Theoretically, ORR activity can be related to E_{ads} of O* and OH*, the key intermediates in ORR. $E_{ads}(O^*)$ and $E_{ads}(OH^*)$, which are indicators of the oxophilicity of the materials, can describe the degrees of reaction barriers in the rate-determining hydrogenation steps for ORR.[2b,2d,8] The most stable $E_{ads}(O^*)$ and $E_{ads}(OH^*)$ on M@Pt (M core/Pt surface) and Pt@M (Pt core/M surface) are examined (Table S3 and Figure S6) and compared with those on pure Pt surface (Figure S7). A larger or less negative E_{ads} value than pure Pt surface suggests a weaker absorption and better modification of the alloy for ORR. Pt@Au can effectively weaken the adspecies bonding due to the less activity of Au through ensemble effect; yet the Au@Pt shows negligible effect on the E_{ads}. Moreover, the alloying of Pd on the E_{ads} is insignificant because of similar chemical (activity) and physical (atomic radius) properties of Pd and Pt. For Ag alloying, the ensemble effect of surface Ag can weaken $E_{ads}(O^*)$, but not the $E_{ads}(OH^*)$, attributable to that Ag is more active to OH*, but less active to O* than Pt, i.e. stronger $E_{ads}(OH^*)$ and weaker $E_{ads}(O^*)$ are found on pure Ag(111) than Pt(111).[9] $E_{ads}(OH^*)$, on the other hand, is reduced by subsurface Ag.

These computational results can be utilized to clarify the experimental observation in Figure 3, which summaries the MA before and after ADT and the degrees of modification on oxophilicity,

$$\Delta E_{ads}(O^* \text{or } OH^*) = E_{ads,\,sample}(O^* \text{or } OH^*) - E_{ads,\,Pt}(O^* \text{or } OH^*) \quad (1)$$

$\Delta E_{ads}(O^* \text{ or } OH^*)$ for the PtM follows the trend Au > Ag > Pd, suggesting that the highest MA for PtAu NRs corresponds to that surface Au can effectively demote the oxophilicity and improve the activity. On the other hand, the results from ADT experiments can be rationalized from the calculation of segregation energies, which are the energy requiring to swap surface Pt and subsurface M. The segregation energies for clean, E_{seg}(clean), and OCS*-adsorbed alloys, $E_{seg}(OCS^*)$, are defined as

$$E_{seg}(\text{clean}) = E_{M\text{-}subsurface}(Pt) - E_{M\text{-}surface}(Pt), \quad (2)$$

$$E_{seg}(OCS^*) = E_{M\text{-}subsurface}(Pt\text{-}OCS^*) - E_{M\text{-}surface}(Pt\text{-}OCS^*) \quad (3)$$

in which $E_{M\text{-}subsurface}$ and $E_{M\text{-}surface}$ are the energies for dopant M in the subsurface and on the surface, respectively. Positive and negative E_{seg} indicate that M is more stable on the surface (Pt@M) and in the

subsurface (M@Pt), respectively. E_{seg}(clean) corresponds to the thermodynamic stability for the as-prepared alloys, before ADT, while $E_{seg}(OCS^*)$ is related to the stability during ORR. Thus, the smaller the difference between these two E_{seg}, the more stability is expected in ADT. As shown in Figure S8, dopant of Au has a positive E_{seg}(clean) (x-axis), 1.13 eV and is thermodynamically stable on the surface to form Pt@Au. The result agrees with the experimental observation[3b] and confirms that the stable surface Au can effectively improve the activity in our ORR experiment exhibited in Figure 2. Moreover, dopant of Pd has a negative value (-0.16 eV), implying that Pd@Pt is the preferential form. Interestingly, the negligible $E_{ads}(Pt)$ (-0.02 eV) for dopant Ag indicates that Ag has no preferential sites and can ideally dissolve in its alloy with Pt. In the comparison of $E_{seg}(OCS^*)$ along the y axis, dopants of Au and Pd have a negative and positive $E_{seg}(OCS^*)$, respectively, for all OCS*. In order to get better understanding of E_{seg}, Figure 3 summaries the E_{seg} (clean) and E_{seg} (OCS*) for Pt@M samples. The significant differences in the E_{seg} (clean) and E_{seg} (OCS*) suggest that those OCS* likely push down Au to the subsurface and pull out Pd to the surface to destabilize their alloys. Thus, a surface segregation of Pt and Pd for PtAu and PtPd alloys, respectively, when exposing to OCS* in ORR results in this significant performance decay after ADT. On the contrary, for Ag alloying, since their OH* and OOH* have positive $E_{seg}(OCS^*)$ and O* and O_2^* have negative ones as displayed in Figure S8, the resulting $E_{seg}(OCS^*)$ for the adspecies on PtAg alloy can balance the swap between surface and subsurface elements. As a result, E_{seg} (clean) and E_{seg} (OCS*) for PtAg shown in Figure 3 is almost the same and PtAg shows the smallest activity decay after ADT.

In summary, Pt_3M NRs with an aspect ratio of 4.0 have been prepared to study their ORR activity and stability by electrochemical measurement and DFT calculations. The ORR activity of Pt_3M NRs is related to the degrees of modification on oxophilicity (ΔE_{ads}), which is the difference between $E_{ads}(O^* \text{ or } OH^*)$ for Pt and its alloys. TPR and DFT results suggest that the modification effect of Pd alloying is insignificant, in which the reduction temperature in TPR is 290 K and the $\Delta E_{ads}(O^*)$ is -0.11 eV. On the contrary, Au can modify the Pt surface obviously so the reduction temperature is as low as 220 K and $\Delta E_{ads}(O^*)$ is 0.47 eV. However, due to the OCS* induced Pt surface segregation, the structure of PtAu becomes unstable during ADT, deteriorating ORR. As a result, although the ΔE_{ads} of PtAg is not as high as that of PtAu, the structure is relative stable with or without OCS*, promoting the ORR stability with a decay of 9 % during ADT.

Acknowledgement

Notes and references

[a] Institute of Materials Science and Engineering, National Central University, Taoyuan 320, Taiwan
[b] Department of Chemistry, National Taiwan Normal University, Taipei 116, Taiwan
[c] Green Energy and Environment Research Laboratories, Industrial Technology Research Institute, Hsinchu 310, Taiwan
[d] Graduate Institute of Materials Science and Green Energy Engineering, National Formosa University, Yunlin 632, Taiwan
[e] Department of Engineering and System Science, National Tsing-Hua University, Hsinchu 300, Taiwan

† Electronic Supplementary Information (ESI) available: [ICP, TGA, XRD, EXAFS,TPR, XPS, DFT results]. See DOI: 10.1039/c000000x/

1. a)H. S. Chen, Y. T. Liang, T. Y. Chen, Y. C. Tseng, C. W. Liu, S. R. Chung, C. T. Hsieh, C. E. Lee and K. W. Wang, *Chem. Commun.* 2014, **50**, 11165. b) X. Sun, D. Li, Y. Ding, W. Zhu, S. Guo, Z. L. Wang and S. Sun, *J. Am. Chem. Soc.* 2014, **136**, 5745. c) B. Lim, M. Jiang, P. H. C. Camargo, E. C. Cho, J. Tao, X. Lu, Y. Zhu and Y. Xia, *Science*, 2009, **324**, 1302. d) Y. Lu, Y. Jiang and W. Chen, *Nano Energy*, 2013, **2**, 836.

2. a) D. Cheng and W. Wang, Nanoscale, 2012, 4, 2408. b) D. Cheng, X. Qiu and H. Yu, *Phys. Chem. Chem. Phys.* 2014, **16**, 20377. c) Y. S. Kim, S. H. Jeon, A. Bostwick, E. Rotenberg, P. N. Ross, V. R. Stamenkovic, N. M. Markovic, T. W. Noh, S. Han and B. S. Mun, *Adv. Energy Mater.* 2013, **3**, 1257. d) V. R. Stamenkovic, B. Fowler, B. S. Mun, G. Wang, P. N. Ross, C. A. Lucas and N. M. Markovic, *Science* 2007, **315**, 493. e)J. Greeley, I. E. L. Stephens, A. S. Bondarenko, T. P. Johansson, H. A. Hansen, T. F. Jaramillo, J. Rossmeisl, I. Chorkendorff and J. K. Nørskov, *Nature Chem.* 2009, **1**, 552. f) S. Alayoglu, A. U. Nilekar, M. Mavrikakis and B. Eichhorn, *Nature Mater.* 2008, **7**, 333.

3. a) J. Zhang, K. Sasaki, E. Sutter and R. R. Adzic, *Science,* 2007, **315**, 220. b) B. N. Wanjala, J. Luo, R. Loukrakpam, B. Fang, D. Mott, P. N. Njoki, M. Engelhard, H. R. Naslund, J. K. Wu, L. Wang, O. Malis and C. J. Zhong, *Chem. Mater.* 2010, **22**, 4282.
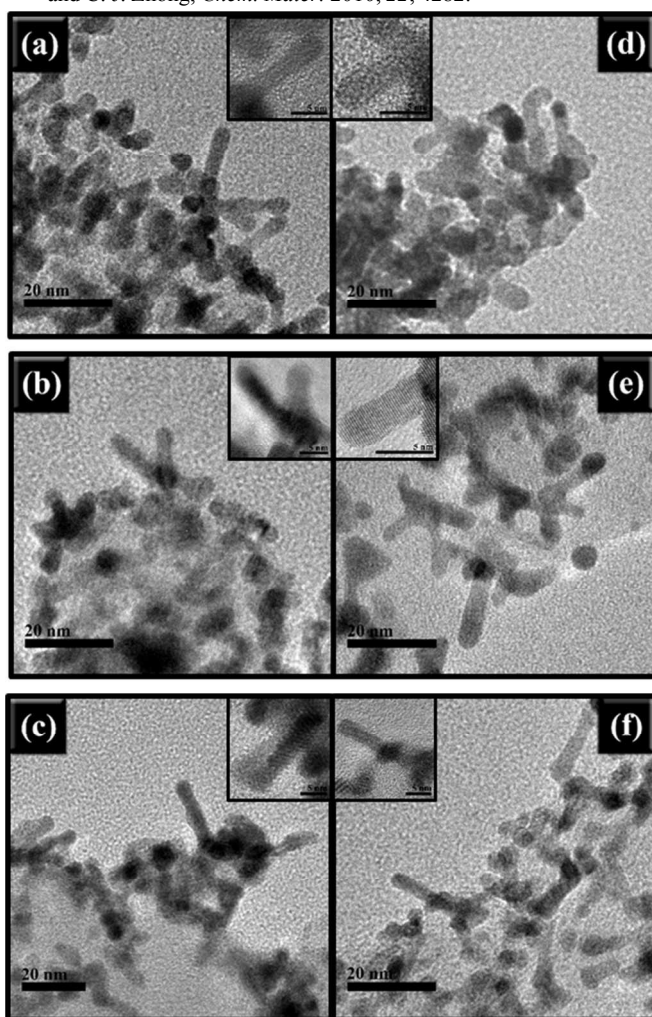
4. a) D. M. Cleperley and B. J. Alder, *Phys. Rev. Lett.*, 1980, **45**, 566. b)J. P. Perdew and Y. Yang, *Phys. Rev. B* 1992, **45**, 244.

5. a) G. Kresse and J. Hafner, *Phys. Rev. B*, 1993, **47**, 558. b) G. Kresse and J. Hafner, *Phys. Rev. B*, 1994, **49**, 1425. c) G. Kresse and J. Furthmüller, *Phys. Rev. B*, 1996, **54**, 11169.

6. a)C. W. Liu, Y. C. Wei, C. C. Liu and K. W. Wang, *J. Mater. Chem.* 2012, **22**, 4641. b) T. H. Yeh, C. W. Liu, H. S. Chen and K. W. Wang, *Electrochem. Commun.* 2013, **31**, 125. c) Y. C. Tseng, H. S. Chen, C. W. Liu, T. H. Yeh and K. W. Wang, *J. Mater. Chem. A* 2014, **2**, 4270.

7. a) Y. C. Wei, C. W. Liu and K. W. Wang, *Chem. Commun.* 2011, **47**, 11927. b) C. W. Liu, Y. C. Wei and K. W. Wang, *J. Phys. Chem. C* 2011, **115**, 8702. c) C. W. Chou, S. Chu, H. J. Chiang, C. Y. Huang, C. J. Lee, S. R. Sheen, T. P. Perng and C. T. Yeh, *J. Phys. Chem. B*, 2001, **105**, 9113.

8. V. Stamenkovic, B. S. Mun, K. J. J. Mayrhofer, P. N. Ross, N. M. Markovic, J. Rossmeisl, J. Greeley and J. K. Norskov, *Angew. Chem. Int. Ed.* 2006, **45**, 2897.

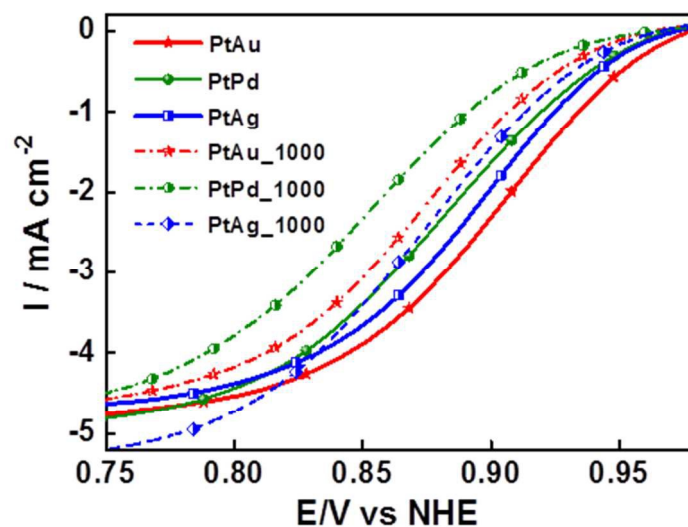9. S. C. Huang, C. H. Lin and J. H. Wang, *J. Phys. Chem. C* 2010, **114**, 9826.

Figure 2. LSV results obtained in O_2-saturated 0.5 M $HClO_4$ before and after 1000 cycles of ADT for PtM NRs.

Figure 1. HRTEM micrographs of catalysts before and after ADT for PtAu (a) and (d), PtPd (b) and (e), PtAg (c) and (f), respectively
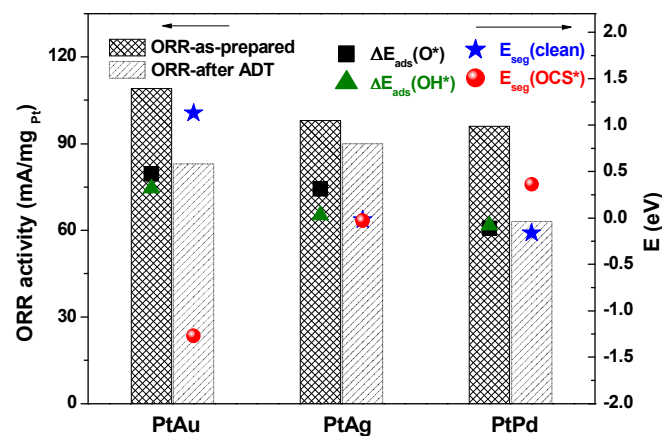

Fig. 3. The comparison in $\Delta E_{ads}(O*)$, $\Delta E_{ads}(OH*)$, $E_{seg}(clean)$, $E_{seg}(OCS*)$ and ORR activity before and after 1000 cycles of ADT for PtM alloys.

ChemComm Accepted Manuscript